Inorg. Chem. **2002**, *41*, 4275–4285

Synthesis and Characterization of the $SO_2N_3^-$, $(SO_2)_2N_3^-$, and $SO_3N_3^-$ Anions†

Karl O. Christe,*,‡,§ Jerry A. Boatz,‡ Michael Gerken,§ Ralf Haiges,§ Stefan Schneider,§ Thorsten Schroer,§ Fook S. Tham,|| Ashwani Vij,‡ Vandana Vij,‡ Ross I. Wagner,§ and William W. Wilson‡

Propulsion Sciences and Advanced Concepts Division, Air Force Research Laboratory (AFRL/PRS), Edwards AFB, California 93524, Loker Hydrocarbon Research Institute and Department of Chemistry, University of Southern California, Los Angeles, California 90089, and University of California, Riverside, California 92521

Received March 7, 2002

SO_2 solutions of azide anions are bright yellow, and their Raman spectra indicate the presence of covalently bound azide. Removal of the solvent at −64 °C from CsN_3 or $N(CH_3)_4N_3$ solutions produces yellow $(SO_2)_2N_3^-$ salts. Above −64 °C, these salts lose 1 mol of SO_2, resulting in white $SO_2N_3^-$ salts that are marginally stable at room temperature and thermally decompose to the corresponding azides and SO_2. These anions were characterized by vibrational and ^{14}N NMR spectroscopy and theoretical calculations. Slow loss of the solvent by diffusion through the walls of a sealed Teflon tube containing a sample of $CsSO_2N_3$ in SO_2 resulted in white and yellowish single crystals that were identified by X-ray diffraction as $CsSO_2N_3 \cdot CsSO_3N_3$ with $a = 9.542(2)$ Å, $b = 6.2189(14)$ Å, $c = 10.342(2)$ Å, and $\beta = 114.958(4)°$ in the monoclinic space group $P2_1/m$, $Z = 2$, and $Cs_2S_2O_5 \cdot Cs_2S_2O_7 \cdot SO_2$, respectively. Pure $CsSO_3N_3$ was also prepared and characterized by vibrational spectroscopy. The S–N bond in $SO_2N_3^-$ is much weaker than that in $SO_3N_3^-$, resulting in decreased thermal stability, an increase in the S–N bond distance by 0.23 Å, and an increased tendency to undergo rotational disorder. This marked difference is due to SO_3 being a much stronger Lewis acid (pF^- value of 7.83) than SO_2 (pF^- value of 3.99), thus forming a stronger S–N bond with the Lewis base N_3^-. The geometry of the free gaseous $SO_2N_3^-$ anion was calculated at the RHF, MP2, B3LYP, and CCSD(T) levels. The results show that only the correlated methods correctly reproduce the experimentally observed orientation of the SO_2 group.

Introduction

Sulfur dioxide is a very interesting molecule. It not only serves as a very useful inorganic solvent but also exhibits a rich reaction chemistry. In addition to being a ligand with at least 9 different bonding modes,[1] it is also amphoteric and can act either as an electron donor (Lewis base) or acceptor (Lewis acid) molecule. As a donor, it can coordinate through its free valence electron pairs on either sulfur or oxygen. A typical example for the latter case is the oxygen-bridged adduct between SbF_5 and SO_2.[2] As an acceptor, SO_2 likes to expand its coordination number around sulfur from three to four. Typical examples for compounds in which SO_2 acts as an acceptor are the SO_2X^- anions, where X^- stands for a halide or pseudo-halide ion.[3]

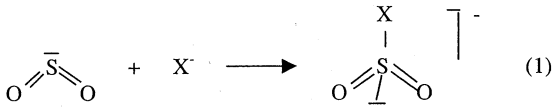

(1)

During reactions, aimed at the metathetical synthesis of $N_5^+N_3^-$, the yellow color of the solutions of colorless N_3^- in colorless SO_2 raised our curiosity. This is in marked

* To whom correspondence should be addressed. E-mail: karl.christe@edwards.af.mil.

† This paper is dedicated to Professor Dieter Naumann on the occasion of his 60th birthday.

‡ Air Force Research Laboratory.
§ University of Southern California.
|| UC Riverside.

(1) Greenwood, N. N.; Earnshaw, A. *Chemistry of the Elements*, 2nd ed.; Butterworth-Heinemann: Oxford, 1998; pp 721−746.
(2) Bacon, J.; Dean, P. A. W.; Gillespie, R. J. *Can. J. Chem.* **1969**, *47*, 1655.
(3) Kornath, A.; Blecher, O.; Ludwig, R. *J. Am. Chem. Soc.* **1999**, *121*, 4019 and references therein.

10.1021/ic020183l CCC: $22.00
Published on Web 07/18/2002

contrast to solutions of N_3^- in other polar solvents, such as water, that are colorless. Therefore, the SO_2/N_3^- system was studied in more detail. The results from this study were presented at the 13th European Symposium on Fluorine Chemistry,[4] and a full account of this work is given in this paper. Our original report[4] provided the first evidence for the existence of the azidosulfite anion and was recently confirmed by an independent crystal structure determination of $[N(CH_3)_4]^+[SO_2N_3]^-$.[5] Despite many known sulfur−nitrogen compounds,[1] including sulfuryl diazide[6] and azidosulfates,[7−12] no other reports on azidosulfites were found in the literature.

The $SO_3N_3^-$ anion has previously been prepared by (a) the direct reaction between SO_3 and NaN_3;[8] (b) the reaction of H_2NNHSO_3H and KNO_2;[7] (c) the reaction of [Na]-[SO_3Cl] and N_3^-;[9,12] and (d) the reaction of $S_2O_6N_3^-$ with KOH/NaOH.[10] Despite this diversity of available synthetic routes, the $SO_3N_3^-$ anion had been characterized only by elemental analyses and infrared spectroscopy.

Experimental Section

Caution! Azides are highly endothermic and often can decompose explosively. They should be handled on a small scale with appropriate safety precautions.

Materials and Apparatus. Reactions were carried out in either flamed-out Pyrex glass tubes or Teflon-FEP or -PFA ampules that contained Teflon coated magnetic stirring bars and were closed by stainless steel or Teflon valves. Volatile materials were handled either on a stainless steel/Teflon-FEP vacuum line[13] or a Pyrex glass vacuum line equipped with grease-free Kontes glass-Teflon valves. Nonvolatile solids were handled in the dry nitrogen atmosphere of a glovebox. Infrared spectra were recorded on either a Mattson Galaxy 5030 or Midac M Series FT-IR spectrometer using dry powders pressed between AgCl windows in an Econo press (Barnes Engineering Co.). Raman spectra were recorded on either a Bruker Equinox 55 FT-RA spectrometer using a Nd:YAG laser at 1064 nm and Pyrex melting point capillaries, glass NMR tubes, or 9 mm Teflon-FEP tubes as sample containers or a Cary Model 83 spectrometer using the 488 nm exciting line of an Ar ion laser. NMR spectra were recorded on a Bruker Avance 400 FT-NMR spectrometer.

The $N(CH_3)_4^+N_3^-$,[14] CsN_3,[15] and $CsSO_3Cl$[16] starting materials were prepared by literature methods. The SO_2 (Air Products, anhydrous grade, 99.9%) was dried over CaH_2. Trimethylsilyl azide (Aldrich, 95%) was condensed from a storage vessel at −35 °C into the reaction vessel at −196 °C.

Preparation of $M^+SO_2N_3^-$ [M = Cs or $N(CH_3)_4$]. In a typical experiment, a 5 mm Pyrex glass NMR tube, closed by a concentric, grease-free Teflon valve (Wilmad Glass Co.), was loaded with CsN_3 (1.335 mmol) in the glovebox. The tube was attached to the Pyrex vacuum line and evacuated; then, anhydrous SO_2 (0.765 mL) was condensed into the tube at −196 °C. The mixture was warmed to room temperature, and the CsN_3 dissolved giving a yellow solution. In the presence of traces of moisture, a small amount of a white precipitate formed that was identified by its infrared and Raman spectra as $Cs_2S_2O_5$.[17] The tube and its contents were cooled to −22 °C, and the SO_2 solvent was pumped off in a dynamic vacuum, leaving behind a white solid (322.0 mg, weight calculated for 1.335 mmol of $CsSO_2N_3$ = 319.1 mg).

Preparation of $M^+(SO_2)_2N_3^-$ [M = Cs or $N(CH_3)_4$]. In a manner similar to that used for the preparation of $CsSO_2N_3$, CsN_3 (1.346 mmol) was loaded into a Pyrex NMR tube equipped with a glass-Teflon valve, and anhydrous SO_2 (0.769 mL) was added in vacuo to the tube at −196 °C. After warming to room temperature to dissolve all the CsN_3, the tube was cooled to −64 °C, and the SO_2 was removed slowly in a dynamic vacuum for 4 h. The nonvolatile residue consisted of a yellow solid (406 mg, weight calculated for 1.346 mmol of $Cs(SO_2)_2N_3$ = 407.9 mg).

Preparation of $CsSO_3N_3$. Inside a drybox, a glass vessel, equipped with a Kontes glass-Teflon valve and a Teflon-coated stirring bar, was loaded with $CsSO_3Cl$ (2.383 mmol). On a glass vacuum line, $(CH_3)_3SiN_3$ (8.940 mmol) was distilled onto the solid at −196 °C and allowed to warm to room temperature. After stirring the suspension for 2 days, volatiles were removed at room temperature yielding a white solid. Raman spectroscopic characterization of the solid revealed the presence of $CsSO_3Cl$ and $CsSO_3N_3$. Four additional cycles of adding fresh $(CH_3)_3SiN_3$, followed by removal of all volatiles at room temperature while monitoring the progress of the reaction by Raman spectroscopy, resulted in a quantitative yield of pure $CsSO_3N_3$.

Crystal Structure Determination of $CsSO_2N_3 \cdot CsSO_3N_3$. About 0.5 mL of SO_2 was condensed onto anhydrous CsN_3 in a 4 mm FEP NMR tube that was then evacuated at −196 °C and heat-sealed. The yellowish solution was allowed to stand for several weeks during which time SO_2 diffused slowly through the walls of the tube, and a mixture of diffraction-quality, prismatic, clear, colorless (compound **1**, $CsSO_2N_3 \cdot CsSO_3N_3$), and pale yellow (compound **2**, $Cs_2S_2O_5 \cdot Cs_2S_2O_7 \cdot SO_2$) crystals was formed. The FEP tube was then cut open under a stream of cold N_2 gas at approximately −80 °C, and the crystalline contents were dropped into the lip of a low temperature crystal-mounting apparatus. A Nylon Cryoloop, attached to a magnetic base, was used to trap a crystal having the dimensions 0.10 × 0.27 × 0.52 mm^3, using PFPE (perfluoropolyether) oil, and to mount it on the magnetic goniometer. The single-crystal diffraction data were collected on a Bruker 3-circle platform diffractometer, equipped with a SMART[18] CCD (charge coupled device) detector with the χ-axis fixed at 54.74°, and using Mo Kα radiation (λ = 0.71073 Å) from a fine-focus tube. This diffractometer was equipped with an LT-3 apparatus for low temperature data collection using controlled liquid nitrogen boil off. Cell constants were determined from 90 30-s frames at

(4) Vij, A.; Wilson, W.; Sheehy, J.; Boatz, J.; Gerken, M.; Schneider, S.; Schroer, T.; Haiges, R.; Wagner, R.; Tham, F.; Christe, K. Presented at the 13th European Symposium on Fluorine Chemistry, Bordeaux, France, July 15−20, 2001; Paper B7.
(5) Kornath, A.; Blecher, O.; Ludwig, R. *Z. Anorg. Allg. Chem.* **2002**, *628*, 183.
(6) Curtius, T.; Schmidt, F. *Ber. Dtsch. Chem. Ges.* **1922**, *55*, 1571.
(7) Traube, W.; Vockerodt, A. *Ber. Dtsch. Chem. Ges.* **1914**, *47*, 943.
(8) Beck, G. *J. Prakt. Chem. (Leipzig)* **1940**, *156*, 227.
(9) Elsner, H.; Ratz, H. German Patent 886,298, 1953.
(10) Lehmann, H. A.; Holznagel, W. *Z. Anorg. Allg. Chem.* **1958**, *293*, 314.
(11) Ruff, J. K. *Inorg. Chem.* **1965**, *4*, 567.
(12) Shozda, R. J.; Vernon, J. A. *J. Org. Chem.* **1967**, *32*, 2876.
(13) Christe, K. O.; Wilson, W. W.; Schack, C. J.; Wilson, R. D. *Inorg. Synth.* **1986**, *24*, 39.
(14) Christe, K. O.; Wilson, W. W.; Bau, R.; Bunte, S. W. *J. Am. Chem. Soc.* **1992**, *114*, 3411.
(15) Gerken, M.; Schneider, S.; Schroer, T.; Christe, K. O. *Z. Anorg. Allg. Chem.*, in press.
(16) Ciruna, J. A.; Robinson, E. A. *Can. J. Chem.* **1968**, *46*, 1715.
(17) Siebert, H. *Anwendungen der Schwingungsspectroskopie in der Anorganischen Chemie, Anorganische und Allgemeine Chemie in Einzeldarstellungen, VII*; Springer-Verlag: Berlin, 1966; p 102. Herlinger, A. W.; Long, T. V. *Inorg. Chem.* **1969**, *8*, 2661.
(18) *SMART V 4.045, Software for the CCD Detector System*; Bruker AXS: Madison, WI, 1999.

Table 1. ^{14}N NMR Spectra of Aqueous and SO_2 Solutions of MN_3 (M = Na, Cs, or $N(CH_3)_4$) and of MSO_2N_3 (M = Cs or $N(CH_3)_4$) in CH_3NO_2, CH_3CN, or CHF_3 Solution

	chem shift, ppm (line width, Hz)		
compound (solvent)	central nitrogen	terminal nitrogen	area ratio
NaN_3 (H_2O, 20 °C)	−133.5 (18)	−282.2 (60)	1:2
NaN_3[b] (SO_2, 20 °C)	−135.8 weak	not obsd	
CsN_3 (SO_2, 20 °C)	−133.9 (15)	−201.7 (76)	1:2
(SO_2, −25 °C)	−134.3 (19)	−200.1 (150)	1:2
(SO_2, −65 °C)	−134.7 (51)	−198.9 (235)	1:2
$CsSO_2N_3$ (CH_3NO_2, −22 °C)	−132.5 (16)	−209.9 (155)	1:2
$N(CH_3)_4N_3$[d] (H_2O, 22 °C)	−133.4 (18)	−281.0 (58)	1:2
$N(CH_3)_4N_3$[d] (SO_2, −65 °C)	−135.0 (35)	−199.8 (200)	1:2
$N(CH_3)_4SO_2N_3$[a,e] (CH_3CN, −40 °C)	−132.7[f]	−205.3 (140)	*f*
$N(CH_3)_4SO_2N_3$ (CHF_3, −90 °C)[b]	−136.4 weak	not obsd	
$N(CH_3)_4(SO_2)_2N_3 \cdot nSO_2$ (CH_3CN, −40 °C)[c,e]	−133.1[f]	−203.7 (192)	*f*

[a] Clear colorless solution with faint yellow solid. [b] Low solubility. [c] Pale yellow solution with yellow solid. [d] The sharp resonances due to $N(CH_3)_4^+$ were observed at −139.3 (H_2O) and −336.9 ppm (SO_2). [e] Resonances due to CH_3CN and $N(CH_3)_4^+$ were observed at −137.7 (~300 Hz) and −338 ppm, respectively. [f] Not determined because of overlap with solvent resonance.

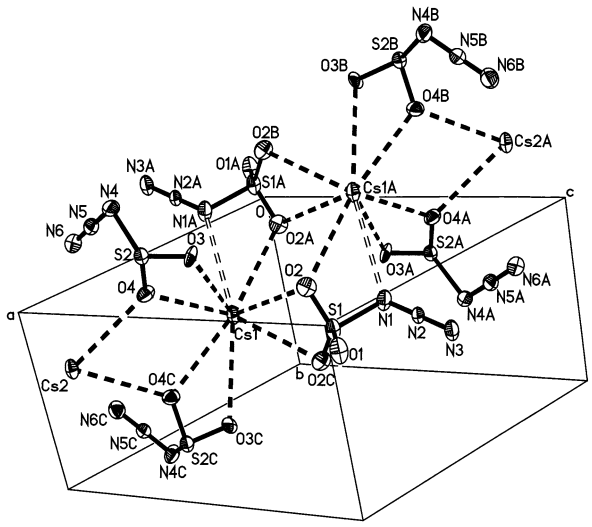

Figure 1. Crystal structure of $CsSO_2N_3 \cdot CsSO_3N_3$.

Table 2. Crystal Data for $CsSO_2N_3 \cdot CsSO_3N_3$ (**1**)

chemical formula	$Cs_2N_6O_5S_2$
fw	494.00
T, °C	−100 (2)
space group	$P2_1/m$ (No.11)
a, Å	9.542(2)
b, Å	6.2189(14)
c, Å	10.342(2)
β, deg	114.958(4)
V, Å^3	556.4(2)
Z	2
ρ_{calcd}, g cm^{-3}	2.949
μ, mm^{-1}	6.939
λ, Å	0.71073
R1,[a] wR2[b] [$I > 2\sigma(I)$]	0.0398, 0.1068
R1,[a] wR2[b] (all data)	0.0416, 0.1085

[a] $R1 = (\sum(F_o - F_c)/F_o)$. [b] $wR2 = [\sum(w(F_o - F_c)^2)/wF_o^2)]^{1/2}$.

−100 °C (**1**) or at −70 °C (**2**). A complete hemisphere of data was collected, using 1271 frames at 30 s/frame at a detector resolution of 512 × 512 pixels, including 50 frames that were collected at the beginning and end of the data collection to monitor crystal decay. The frames were then processed on a PC running on Windows NT software by using the SAINT software[19] to give the *hkl* file corrected for Lp/decay. The absorption correction was performed using the SADABS[20] program. The structures were solved by the direct method, using the SHELX-97 program,[21] and refined by the least-squares method on F^2, SHELXL-97,[22] incorporated in SHELXTL Suite 5.10 for Windows NT.[23] All atoms were refined anisotropically. For the anisotropic displacement parameters, the *U*(eq) is defined as one-third of the trace of the orthogonalized U_{ij} tensor.

Table 3. Atomic Coordinates ($\times 10^4$) and Equivalent Isotropic Displacement Parameters (Å^2 × 10^3) for $CsSO_2N_3 \cdot CsSO_3N_3$

	x	*y*	*z*	*U*(eq)[a]
Cs(1)	6199(1)	2500	3672(1)	38(1)
Cs(2)	10539(1)	2500	1983(1)	39(1)
S(1)	6914(2)	2500	7536(2)	42(1)
S(2)	9094(3)	−2500	3854(2)	40(1)
O(1)	8336(7)	2500	8827(6)	59(2)
O(2)	6625(5)	562(8)	6701(5)	49(1)
O(3)	8278(16)	−3010(20)	4683(12)	47(5)
O(4)	8677(11)	−276(12)	3266(9)	45(2)
O(5)[b]	10543(17)	−3070(30)	3910(30)	45(7)
N(1)	5404(10)	1975(19)	8035(10)	49(4)
N(2)	5694(7)	2500	9245(6)	31(1)
N(3)	5843(12)	3101(19)	10317(11)	51(4)
N(4)	7990(17)	−4208(17)	2097(14)	55(3)
N(5)	7791(13)	−3134(14)	1059(12)	40(2)
N(6)	7645(14)	−2130(30)	100(13)	52(5)

[a] *U*(eq) is defined as one-third of the trace of the orthogonalized U_{ij} tensor. [b] O(5) is the minor component of the rotationally disordered $SO_2N_3^-$ anion (see Results and Discussion section) and is not shown in Figure 1.

Theoretical Calculations. Theoretical calculations were carried out on IBM RS/6000 work stations using the GAMESS,[24] Gaussian 98,[25] and ACES II[26] program systems and the restricted Hartree−Fock (RHF),[27] the density functional B3LYP,[28] and the correlated

(19) *SAINT V 4.035*, *Software for the CCD Detector System*; Bruker AXS: Madison, WI, 1999.
(20) *SADABS*, *Program for absorption correction for area detectors*, version 2.01; Bruker AXS: Madison, WI, 2000.
(21) Sheldrick, G. M. *SHELXS-97*, *Program for the Solution of Crystal Structure*; University of Göttingen: Göttingen, Germany, 1997.
(22) Sheldrick, G. M. *SHELXL-97*, *Program for the Refinement of Crystal Structure*; University of Göttingen: Göttingen, Germany, 1997.
(23) *SHELXTL 5.10 for Windows NT*, *Program library for Structure Solution and Molecular Graphics*; Bruker AXS: Madison, WI, 1997.
(24) Schmidt, M. W.; Baldridge, K. K.; Boatz, J. A.; Elbert, S. T.; Gordon, M. S.; Jensen, J. H.; Koseki, S.; Matsunaga, N.; Nguyen, K. A.; Su, S. J.; Windus, T. L.; Dupuis, M.; Montgomery, J. A. *J. Comput. Chem.* **1993**, *14*, 1347−1363.
(25) Frisch, M. J.; Trucks, G. W.; Schlegel, H. B.; Scuseria, G. E.; Robb, M. A.; Cheeseman, J. R.; Zakrzewski, V. G.; Montgomery, J. A., Jr.; Stratmann, R. E.; Burant, J. C.; Dapprich, S.; Millam, J. M.; Daniels, A. D.; Kudin, K. N.; Strain, M. C.; Farkas, O.; Tomasi, J.; Barone, V.; Cossi, M.; Cammi, R.; Mennucci, B.; Pomelli, C.; Adamo, C.; Clifford, S.; Ochterski, J.; Petersson, G. A.; Ayala, P. Y.; Cui, Q.; Morokuma, K.; Malick, D. K.; Rabuck, A. D.; Raghavachari, K.; Foresman, J. B.; Cioslowski, J.; Ortiz, J. V.; Stefanov, B. B.; Liu, G.; Liashenko, A.; Piskorz, P.; Komaromi, I.; Gomperts, R.; Martin, R. L.; Fox, D. J.; Keith, T.; Al-Laham, M. A.; Peng, C. Y.; Nanayakkara, A.; Gonzalez, C.; Challacombe, M.; Gill, P. M. W.; Johnson, B. G.; Chen, W.; Wong, M. W.; Andres, J. L.; Head-Gordon, M.; Replogle, E. S.; Pople, J. A. *Gaussian 98*, revision A.6; Gaussian, Inc.: Pittsburgh, PA, 1998.
(26) Stanton, J. F.; Gauss, J.; Watts, J. D.; Nooijen, M.; Oliphant, N.; Perera, S. A.; Szalay, P. G.; Lauderdale, W. J.; Gwaltney, S. R.; Beck, S.; Balkova, A.; Bernholdt, D. E.; Baeck, K. K.; Rozyczko, P.; Sekino, H.; Hober, C.; Bartlett, R. J. *ACES II*, *Quantum Theory Project*; University of Florida: Gainesville, FL. Integral packages included are VMOL (Almlof, J.; Taylor, P. R.), BPROPS (Taylor, P. R.), and ABACUS (Helgaker, T.; Jensen, H. J. A.; Jorgensen, P.; Olsen, J.; Taylor, P. R.).

Table 4. Most Important Bond Lengths [Å] and Angles [deg] of the $SO_2N_3^-$ Anion in Its Cs^+ Salt Compared to Those in $[N(CH_3)_4]^+SO_2N_3^-$ and the Calculated[a] Values

	calcd				obsd	
	RHF	B3LYP	MP2	CCSD(T)	$Cs^+SO_2N_3^-$	$[N(CH_3)_4]^+SO_2N_3^-$ [b]
			Bond Distances (Å)			
S−N	1.907	2.226	2.356	2.198	1.981(12)	2.005(2)
S−O[c]	1.464	1.492	1.492	1.494	1.410(10)[e]	1.453(2)
S−O[d]	1.462	1.490	1.491	1.493	1.495(8)	1.457(2)
$N_\alpha-N_\beta$	1.205	1.207	1.223	1.222	1.209(16)	1.214(2)
$N_\beta-N_\gamma$	1.113	1.169	1.205	1.182	1.130(16)	1.144(2)
			Bond Angles (deg)			
O−S−N[d]	101.46	99.21	99.94	99.01	100.1(5)	96.82(8)
O−S−N[c]	102.09	102.42	102.24	101.46	102.7(11)[f]	100.87(9)
S− $N_\alpha-N_\beta$	112.0	110.29	106.81	108.67	110.0(8)	110.22(14)
$N_\alpha-N_\beta-N_\gamma$	178.9	179.16	179.32	179.37	178.2(15)	178.6(2)
O−S−O	112.6	114.58	115.58	114.90	111.1(9)[e]	112.72(10)

[a] A 6-31+G(d) basis set was used for all calculations. [b] Data from ref 2. [c] Oxygen atom that is approximately perpendicular to the plane of the N_3S fragment. [d] Oxygen atom that is approximately in plane with the N_3S fragment. [e] Average value from disordered positions. [f] Taken from the major component of the disordered oxygen position.

MP2[29] and single- and double-excitation coupled cluster methods,[30] including a noniterative treatment of connected triple excitations.[31]

Results and Discussion

SO_2/N_3^- System. In common solvents, such as water, the N_3^- anion dissolves without color and retains its centrosymmetric, linear $D_{\infty h}$ structure, as shown by its spectroscopic properties. For example, an aqueous NaN_3 solution exhibits in the Raman spectrum only the symmetric N_3^- stretching mode at 1340 cm^{-1} and in the ^{14}N NMR spectrum two resonances at −282.2 and −133.5 ppm, respectively, with an area ratio of 2:1. By contrast, a solution of CsN_3 in liquid SO_2 is intense yellow and exhibits a strong Raman band at 2016 cm^{-1}, and its ^{14}N resonance for the two terminal nitrogen atoms is deshielded by 80 ppm relative to that of the free ion (Table 1). The ^{14}N NMR spectrum of a 1:1 mixture of CsN_3 and SO_2 in CH_3NO_2 solution exhibits also two resonances at $\delta = -209.9$ and −132.5 ppm, respectively, with an area ratio of 2:1. These chemical shifts are similar to those of −201.7 and −133.9 ppm observed for the SO_2 solution. The observation of a single resonance for the terminal nitrogen atoms, even for solutions of the 1:1 and 1:2 adducts in CH_3CN at low temperatures, and the weak temperature dependence of the chemical shifts indicate that the SO_2 groups in azidosulfites undergo rapid exchange on the NMR time scale.

These observations are strong indications that SO_2 forms adducts with the azide anion. The combining ratios of N_3^- with SO_2 were studied both experimentally and by theoretical calculations. It was found that at −64 °C SO_2 forms with $Cs^+N_3^-$ yellow 2:1 adducts that at about −30 °C lose 1 mol of SO_2 and yield white 1:1 adducts. The 1:1 adducts are marginally stable at room temperature and, when heated to about 60 °C, decompose to pure N_3^- and SO_2. The corresponding $N(CH_3)_4^+$ salts are thermally somewhat less stable. The underlying chemistry can be used for the conversion of insoluble halides, such as fluoride, into azide. For example, CsF is insoluble in most organic solvents and reacts only incompletely with reagents such as trimethylsilyl azide. It reacts, however, with SO_2 forming soluble SO_2F^-. The fluoride in SO_2F^- can then readily be exchanged for azide using trimethylsilyl azide, resulting in the formation of $SO_2N_3^-$. The latter is then thermally decomposed to give pure azide and SO_2.[15] During the pyrolysis of $SO_2N_3^-$, no evidence was obtained for any N_2 elimination before the loss of all the SO_2 which might have offered a potential synthesis for NSO_2^- salts.[32−34] In the presence of small amounts of moisture, colorless cesium salts of $S_2O_5^{2-}$ and $S_2O_7^{2-}$ can be formed as insoluble byproducts.[35]

$$H_2O + SO_2 \rightarrow H_2SO_3 \quad (2)$$

$$SO_2 + H_2SO_3 + 2CsN_3 \rightarrow Cs_2S_2O_5\downarrow + 2HN_3 \quad (3)$$

As SO_2 has very little vapor pressure below −64 °C, the isolation of well-defined adducts containing more than two SO_2 molecules per N_3^- could not be studied experimentally.

In agreement with the experimental observations, the theoretical calculations show that SO_2 can form stable 1:1 and 2:1 adducts with N_3^-. In the 1:1 adduct, the SO_2

(27) Levine, I. N. *Quantum Chemistry*, 3rd ed.; Allyn and Bacon: Boston, 1983, p 373.
(28) The B3LYP functional uses a three-parameter exchange functional of Becke (B3) [Becke, A. D. *J. Chem. Phys.* **1993**, *98*, 5648. Stephens, P. J.; Devlin, C. F.; Chabalowski, C. F.; Frisch, M. J. *J. Phys. Chem.* **1994**, *98*, 11623.] and the Lee, Yang, and Parr (LYP) correlation gradient-corrected functional [Lee, C.; Yang, W.; Parr, R. G. *Phys. Rev. B* **1988**, *37*, 785.].
(29) (a) Pople, J. A.; Binkley, J. S.; Seeger, R. *Int. Quantum Chem.* **1976**, *10*, 1. (b) Bartlett, R. J.; Silver, D. M. *Int. Quantum Chem.* **1975**, *9*, 183. (c) Dupuis, M.; Chin, S.; Marquez, A. In *Relativistic and Electron Correlation Effects in Molecules*; Malli, G., Ed.; Plenum: New York, 1994. (d) Frisch, M. J.; Head-Gordon, M.; Pople, J. A. *Chem. Phys. Lett.* **1990**, *166*, 275. (e) Bartlett, R. J.; Stanton, J. F. J. Applications of post-Hartree−Fock methods: A Tutorial. In *Reviews of Computational Chemistry*; Lipkowitz, K. B., Boyd, D. B., Eds.; VCH Publishers: New York, 1994, Vol. V.
(30) Purvis, G. D., III; Bartlett, R. J. *J. Chem. Phys.* **1982**, *76*, 1910.
(31) Raghavachari, K.; Trucks, G. W.; Pople, J. A.; Head-Gordon, M. *Chem. Phys. Lett.* **1989**, *157*, 479.
(32) Roesky, H. W.; Schmieder, W.; Isenberg, W.; Boehler, D.; Sheldrick, G. M. *Angew. Chem., Int. Ed. Engl.* **1982**, *21*, 153. Roesky, H. W.; Panday, K. P.; Krebs, B.; Dartmann, M. *J. Chem. Soc., Dalton Trans.* **1984**, 2271.
(33) Chivers, T.; Schmidt, K. J.; McIntyre, D. D.; Vogel, H. J. *Can. J. Chem.* **1989**, *67*, 1788.
(34) Morgon, N. H.; Linnert, H. V.; Riveros, J. M. *J. Phys. Chem.* **1995**, *99*, 11667.
(35) Seel, F.; Mueller, E. *Chem. Ber.* **1955**, *88*, 1747.

molecule is attached to one of the terminal nitrogens of the azide anion. This is in accord with the negative charges in N_3^- residing mainly on the terminal nitrogen atoms, thus making them the better donors. The N−S bond of the

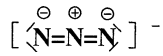

resulting adducts is relatively long, varies strongly with the computational level, and ranges for the 1:1 adduct from 1.91 Å at the RHF level to 2.36 Å at the MP2 level.

For the 2:1 adducts, the two SO_2 groups could reside on either the same or both terminal nitrogen atoms. The energy differences between the 1,1-adduct (rN−S = 2.47 Å at MP2) and the 1,3-adduct (rN−S = 2.56 Å) are predicted to be small, that is, less than 1 kcal/mol at the MP2 and less than 4 kcal/mol at the B3LYP level of theory in favor of the 1,1-adduct.

On the basis of our calculations, the addition of a third SO_2 molecule to the 1,1 adduct lengthens the two original 1,1 N−S bonds to 2.52 Å, but the third N−S bond to the other terminal nitrogen is much weaker at 2.87 Å. Similarly, the addition of a fourth SO_2 molecule affects the three original N−S bonds relatively little; the two geminal N−S bonds at 2.54 Å become slightly longer, and the third N−S bond at 2.80 Å becomes slightly shorter. However, the fourth N−S bond at 3.19 Å becomes much longer. These calculations at the MP2 level confirm that in the presence of excess SO_2 the N−S bonds become very weak, thus accounting for the observed facile N−S bond breakage on an NMR time scale. A more detailed discussion of the calculated structures will be given in a following section.

The $SO_2N_3^-$ anion can be described as either a donor−acceptor adduct between the Lewis acid SO_2 and the Lewis base N_3^- or, by analogy with many known SO_2X^- (X = halogen or pseudohalogen) anions, as an azidosulfite anion. Whereas either description is acceptable, the description of the higher $(SO_2)_nN_3^-$ adducts as azidopolysulfites is inappropriate because there is no significant interaction between the SO_2 ligands. For the analogous $(SO_3)_nN_3^-$ adducts, azidopolysulfate structures have previously been suggested;[10] however, it appears likely that these SO_3 analogues also contain discrete SO_3 units and not polysulfate anions.

The white crystals (compound **1**), obtained from a sample of $CsSO_2N_3$ in SO_2 solution that was kept in a Teflon NMR tube at room temperature for several weeks, had the composition $CsSO_2N_3 \cdot CsSO_3N_3$. These crystals were stable only at low temperature or under an atmosphere of SO_2 at room temperature. The asymmetric unit in the crystal lattice of **1** shows two cesium, two sulfur, and five oxygen atoms besides six nitrogen atoms forming two azide groups (Figure 1 and Tables 2−4). The cesium and sulfur atoms, and O1 and N2, lie on special positions. The large thermal ellipsoids observed for the N1, N3, N4, N5, and N6 atoms indicate a disorder across the crystallographic mirror plane. These atoms were then moved off the mirror plane and refined which resulted in two disordered azide conformations on the sulfur groups. In $SO_2N_3^-$, the sulfur atom S2 is connected to three oxygen positions with a total occupancy of 2 and,

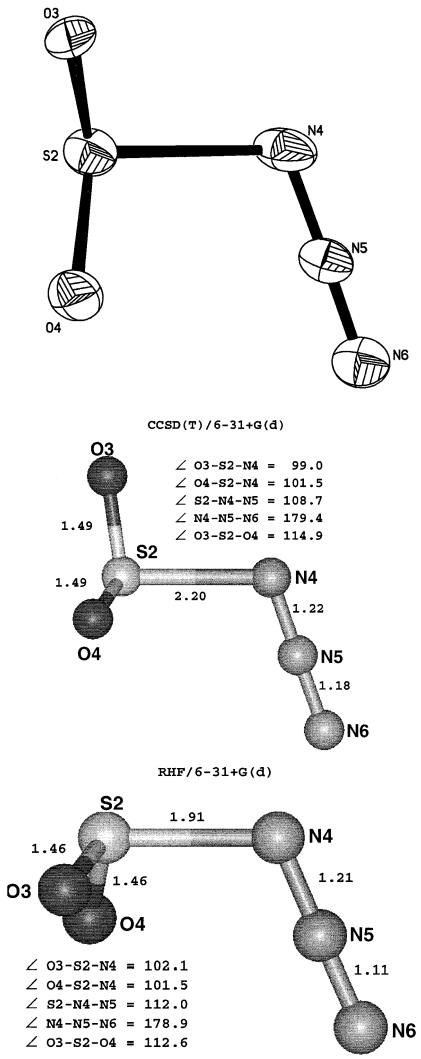

Figure 2. ORTEP plot (30%) of the experimental $SO_2N_3^-$ structure and the structures calculated at the CCSD(T)/6-31+G(d) and RHF/6-31+G(d) levels of theory.

therefore, is attributed to an SO_2 group. The oxygen atoms on S2 exhibit rotational disorder and have refined occupancies for O3 and O5 of 64% and 36%, respectively. A comparison of the geometry found in this study for $SO_2N_3^-$ in its cesium salt (see Figure 2) with that in the ordered $N(CH_3)_4^+$ salt[5] and the theoretical predictions at the correlated level (see Figure 2 and Table 4) shows good agreement and demonstrates that the counterion does not strongly influence the structure of $SO_2N_3^-$.

The $SO_3N_3^-$ anion is also slightly disordered. The N1 and N3 atoms are disordered across the crystallographic symmetry plane through S1, O1, and N2. Figure 3 depicts one of the two disordered components. Furthermore, the rotation of the SO_3 group with respect to the N_3 group deviates from the predictions at the MP2 and B3LYP levels of theory (see Table 5 and Figure 3). In the free gaseous anion, the O1, S1, N1, N2, and N3 atoms are all predicted to be coplanar, with O1 being trans to the azide group, while in the experimental solid-state structure it is cis. Because the calculated energy difference between the cis and trans rotamers is very small because of the weak S−N bond and

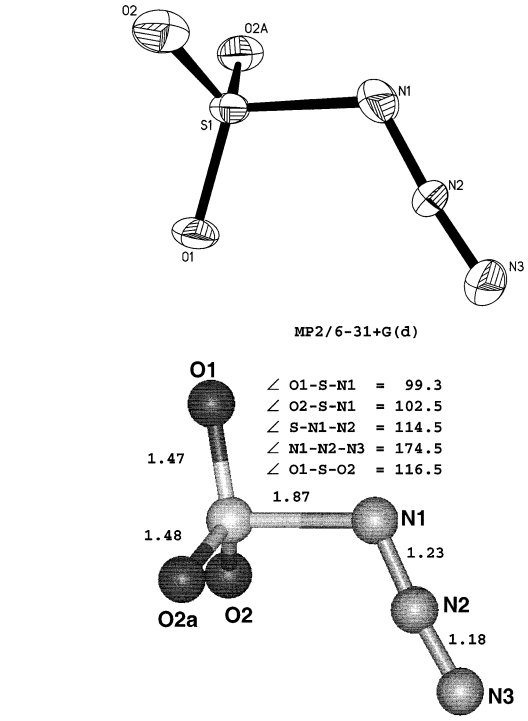

Figure 3. ORTEP plot (30%) of the experimental $SO_3N_3^-$ structure and the structure calculated at the MP2/6-31+G(d) level of theory.

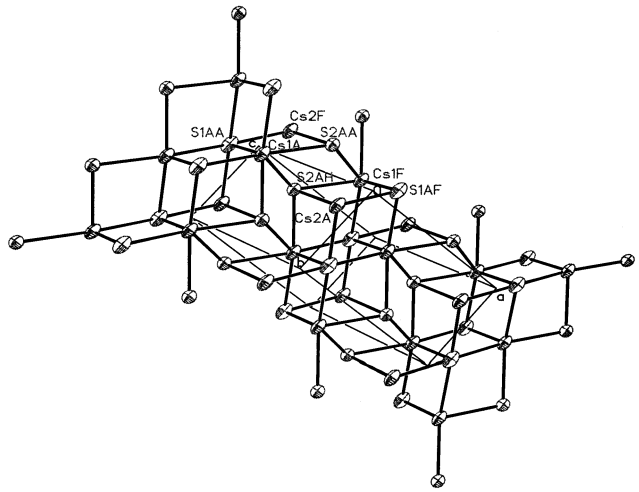

Figure 4. Packing diagram of $CsSO_2N_3 \cdot CsSO_3N_3$ showing the cesium−sulfur network.

its low frequency (33 cm^{-1}) torsion mode, the orientation of the SO_3 group is easily affected by the strong oxygen−cesium interactions in the lattice (see later).

A comparison of the experimental structures of $SO_2N_3^-$ and $SO_3N_3^-$ shows a remarkable difference of 0.23 Å for the S−N distances, that is, 1.981(12) Å for $SO_2N_3^-$ and 1.754(10) Å for $SO_3N_3^-$. The observed difference agrees well with that of 0.32 Å predicted at the B3LYP level and can be rationalized by the large difference in the Lewis acidities of SO_2 and SO_3. On the basis of the Christe/Dixon pF^- scale,[36] SO_2 and SO_3 have pF^- values of 3.99 and 7.83, respectively. If one views the $SO_2N_3^-$ and $SO_3N_3^-$ anions as Lewis acid/Lewis base adducts (see a previous section), it is not surprising that the stronger Lewis acid SO_3 forms the more stable adduct with the azide anion. Because of its longer S−N bond, the $SO_2N_3^-$ anion should undergo SO_n group rotation even more easily than $SO_3N_3^-$. Therefore, one can expect the orientations of the SO_n groups in the $SO_nN_3^-$ anions to vary significantly from one salt to another. The $N_\beta-N_\gamma$ distances at ∼1.13 Å are significantly shorter than the $N_\alpha-N_\beta$ distances at ∼1.21 Å and are characteristic for covalent azides with significant triple and double bond character, respectively. With increasing S−N bond length and a weakening of the $SO_2-N_3^-$ interaction, the $N_\alpha-N_\beta$ and $N_\beta-N_\gamma$ bonds become, as expected, more similar, and their values approach those of the free N_3^- anion.

Table 5. Most Important Bond Lengths [Å] and Angles [deg] of the $SO_3N_3^-$ Anion in Its Cs^+ Salt Compared to the Calculated Values

	calcd		
	B3LYP/6-31+G(d)	MP2/6-31+G(d)	obsd
	Bond Distances (Å)		
S−N	1.876	1.871	1.754(10)
S−O′	1.473	1.472	1.440(5)
$S-O_2$	1.479	1.478	1.447(6)
$N_\alpha-N_\beta$	1.223	1.233	1.207(11)
$N_\beta-N_\gamma$	1.151	1.175	1.120(11)
	Bond Angles (deg)		
O′−S−N	99.59	99.31	92.7(4)
O_2-S-N	102.94	102.47	107.2(4)
$S-N_\alpha-N_\beta$	114.21	114.52	110.0(8)
$N_\alpha-N_\beta-N_\gamma$	175.39	174.48	173.5(10)
$O'-S-O_2$	116.18	116.45	114.9(2)
S−N−N−N	180.00	180.00	180.0
O′−S−N−N	180.00	180.00	180.0

The $CsSO_2N_3 \cdot CsSO_3N_3$ structure exhibits many short contacts indicative of strong interionic interactions. Thus, all the Cs···O distances fall within the range 3.047(6) (Cs2···O1)−3.40(2) (Cs2···O5) Å and are considerably shorter than the sum of their van der Waals radii of about 4.5 Å.[37] The Cs···N contacts of 3.219(13) and 3.305(11) Å, involving the $SO_2N_3^-$ and the $SO_3N_3^-$ groups, respectively, are also significantly shorter than the sum of their van der Waals radii of about 4.54 Å. The S1···Cs2 contact of 3.848-(2) Å is also considerably shorter than the average distance of ∼4.43 Å for the remaining Cs···S contacts.

The short Cs···O contacts mentioned here result in a three-dimensional network of four-membered Cs_2O_2 rings involving alternating SO_3N_3 and SO_2N_3 units (Figure 1). A mean least-squares plane analysis of these two four-membered rings shows that they are twisted by 93.4° with respect to each other. The cesium−sulfur network (Figure 4) forms the basic crystal lattice that is built up of face- and edge-sharing cuboids stacked in a stair-like fashion.

The yellow impurity (**2**) was identified as a double salt of $Cs_2S_2O_5$ and $Cs_2S_2O_7$ with a molecule of SO_2 present as a solvate. The crystal structures of the separate anions have previously been reported,[38−41] and the structure of this ternary compound will be discussed in a forthcoming paper.

Vibrational Spectra and Theoretical Calculations. The vibrational spectra of $CsSO_2N_3$, $N(CH_3)_4SO_2N_3$, $Cs(SO_2)_2N_3$,

(36) Christe, K. O.; Dixon, D. A.; McLemore, D.; Wilson, W. W.; Sheehy, J. A.; Boatz, J. A. *J. Fluorine Chem.* **2000**, *101*, 151.

(37) Bondi, A. *J. Phys. Chem.* **1964**, *68*, 441.

(38) Lindqvist, I. *Acta Crystallogr.* **1957**, *10*, 406.

Table 6. Vibrational Spectra of Solid $[N(CH_3)_4][SO_2N_3]$ and $Cs[SO_2N_3]$ and Assignment of the $SO_2N_3^-$ Anion Bands Based on the Unscaled Frequencies and Intensities Calculated at the RHF, MP2, B3LYP, and CCSD(T) Levels of Theory[a]

vibrational frequencies, cm^{-1}									
calcd for free $SO_2N_3^-$				exptl				assignments	
				$N(CH_3)_4^+$	Cs^+				
RHF	MP2	B3LYP	CCSD(T)	Raman, −65 °C	IR, 22 °C	Raman, 22 °C	Raman, −100 °C	$SO_2N_3^-$	$N(CH_3)_4^+$
				3039(45)					
				3035(40)sh					
				2995(11)sh					
				2981(13)sh					
				2958(36)					
				2923(11)					
				2915(10)					ν(CH) modes
				2883(4)					
				2859(4)					
				2824(2)sh					
				2817(5)					
				2797(3)					
				2019(19)	2036vs	2036(20)	2042(16)	(1333 + 428 + 269)	
2375(1456)[146]	2143(889)[107]	2106(1182)[120]	2043	2014(27)		2013(25)	2018(30)	$\nu_{as}(N_3)$	
				1488(2)					$\nu_2(A_1)$, $\delta_s(CH_3)$
				1469(13)					$\nu_6(E)$, $\delta_{as}(CH_3)$
				1463(15)					
				1417(2)					$\nu_{16}(F_2)$, $\delta_s(CH_3)$
				1404(2)					
				1332(2)	1329m	1330(5)	1333(5)	(2 × 663)	
				1294(2)					$\nu_{17}(F_2)$, CH_3 rock
1411(434)[10]	1239(3)[34]	1350(42)[17]	1291	1272(7)	1272m	1274(13)	1274(14)	$\nu_s(N_3)$	
1289(431)[7.3]	1244(249)[56]	1198(297)[25]	1202	1197(5)	1196s	1190(9)	1188(9)	$\nu_{as}(SO_2)$	
				1188(7)					$\nu_7(E)$, CH_3 rock
				1179(2)					
				1143(2)			1145(1)		
1164(207)[20]	1087(199)[203]	1065(266)[65]	1056	1083(47)	1073s	1077(100)	1078(61)	$\nu_s(SO_2)$	
				1076(20)sh					
				952(12)					$\nu_{18}(F_2)$, $\nu_{as}(CN_4)$
				758(9)					$\nu_3(A_2)$, $\nu_s(CN_4)$
793(10)[10]	586(1)[4]	646(6)[1]	598	665(0+)	662mw	660(3)	663(2)	$\delta(N_3)$ in SN_3 plane	
700(18)[0.1]	550(1)[1]	608(6)[0.3]	549					$\delta(N_3)$ out of SN_3 plane	
607(116)[1.4]	497(33)[4]	504(27)[4]	505	544(4)	547m	540(7)	543(5)	δ_{sciss} (SO_2)	
				460(5)					$\nu_{19}(F_2)$, $\delta(CN_4)$
499(263)[6.4]	329(133)[10]	369(122)[8]	368	405(12)	414ms	420(15)	428(17)	$\delta_s SO_2N$	
				377(2)					$\nu_{12}(F_1)$, $\tau(CH_3)$
352(13)[2.9]	181(11)[12]	220(1)[6]	223	295(10)		309(30)	317(45)	$\tau(SO_2)$	
310(189)[29]	167(38)[17]	181(50)[20]	177	224(100)		258(84)	269(100)	ν(SN)	
150(4.0)[11]	69(4)[11]	106(9)[14]	96	154(28)		169(20)	175(24)	δ_{sciss} (SNN)	
							125sh		
				100(24)		96(100)	103(56)	lattice vibrations	
				86(17)sh		86sh			
				78(31)			78(27)		
17(0.9)[8.4]	30(1)[10]	22(1)[7]	25					$\tau(O_2S-N_3)$	

[a] Bands arising from the FEP sample tube were observed at 735(2) cm^{-1} in the spectrum of the $N(CH_3)_4^+$ salt.

$N(CH_3)_4(SO_2)_2N_3$, and $CsSO_3N_3$ are summarized in Tables 6−8 and Figures 5−7. The assignments were made by comparison with the calculated spectra and are supported by normal coordinate analyses. The correctness of the given mode descriptions was established by the calculated potential energy distributions. All the listed calculations were carried out with a 6-311+G(d) basis set. The calculations at the B3LYP level were also done with 6-311+G(2d) and aug-cc-pvtz basis sets and showed that the choice of the basis set had little influence on the results. For the ease of presentation, the spectra are discussed in the following order: $SO_2N_3^-$, $(SO_2)_2N_3^-$, N_3^- in SO_2 solution, and $SO_3N_3^-$.

$SO_2N_3^-$. The structure of the $SO_2N_3^-$ anion is well established by the crystal structures of its $N(CH_3)_4^+$ [5] and Cs^+ (Figure 2) salts and the results from the theoretical calculations (Figure 2 and Table 4). It must be emphasized that only the calculations at a correlated level duplicate the experimentally observed orientation of the SO_2 group. At the RHF level, the SO_2 group points in the same direction as the azido group. However, the energy difference between the two calculated structures is only about 1 kcal/mol because of the rotational barrier along the N−S bond in $SO_2N_3^-$ (ν = 22 cm^{-1} at the B3LYP level) being even lower than that in $SO_3N_3^-$ (ν = 33 cm^{-1}). The agreement between the observed and the calculated spectra (see Table 6) is satisfac-

(39) Baggio, S. *Acta Crystallogr.* **1971**, *27*, 517.
(40) Wang, Y.; Chen, I.-C. *Acta Crystallogr., Sect. C* **1984**, *40*, 1780.
(41) Hvoslef, J.; Tracy, M. L.; Nash, C. P. *Acta Crystallogr., Sect. C* **1986**, *42*, 353.

Table 7. Vibrational Spectra of $[N(CH_3)_4][(SO_2)_2N_3]$ and $[Cs][(SO_2)_2N_3]$ and Assignments for $(SO_2)_2N_3^-$ Based on the Frequencies and Intensities Calculated at the MP2 and B3LYP Levels of Theory[a,b]

vibrational frequencies, cm^{-1}							
calcd for free $O_2SNNNSO_2^-$		calcd for free $(O_2S)_2NNN^-$		exptl		assignments	
MP2	B3LYP	B3LYP	MP2	$N(CH_3)_4^+$ Raman, −80 °C[a]	Cs^+ Raman, −100 °C	$(O_2S)_2N_3^-$	$N(CH_3)_4^+$
				3052(8)sh			
				3043(12)			
				3037(8)sh			
				2992(13)}			
				2976(5)			$\nu(CH_3)$ modes
				2960(6)			
				2930(10)			
				2903(1)			
				2826(4)			
2096(10)[93]	2076(35)[11]	2125(21)[137]	2102(12)[206]	2028(1)	2028(27)	$\nu_{as}(N_3)$	
				1981(13)	2019(17)		
				1492(1)			$\nu_2(A_1)$, $\delta_s(CH_3)$
				1471(1)			$\nu_6(E)$, $\delta_{as}(CH_3)$
				1455(6)			
				1422(1)			$\nu_{16}(F_2)$, $\delta_s(CH_3)$
				1383(1)			
				1333(13)			
1241(0)[46]	1379(0)[22]	1339(2)[11]	1252(4)[58]	1316(2)	1308(3.6)	$\nu_s(N_3)$	
				1299(5)			$\nu_{17}(F_2)$, CH_3 rock
1236(1)[67]	1243(11)[29]	1235(5)[24]	1242(5)[38]		1273(5)		
1228(8)[13]	1241(0)[17]	1224(5)[24]	1217(0.1)[32]	1250(1)	1246(2)	$\nu_{as}(SO_2)$	
					1223(3)		
				1177(1)			$\nu_7(E)$, CH_3 rock
				1140(100)	1120(100)		
1052(1)[457]	1094(4)[307]	1088(2)[176]	1080(4)[287]	1136(98)	1113(6)	$\nu_s(SO_2)$	
1052(5)[143]	1077(7)[112]	1078(6)[51]	1067(2)[219]	1128(30)	1099(41)		
				1082(1)	1096sh		
				1074(1)			
				956(4)			$\nu_{18}(F_2)$, $\nu_{as}(CN_4)$
				756(6)			$\nu_3(A_2)$, $\nu_s(CN_4)$
563(0)[2]	640(0)[4]	638(0)[2]	563(0.1)[0.6]		644(2)		
546(0)[1]	620(0)[1]	606(0)[2]	502(0.3)[1.4]		617(1.6)		
					546(0.4)		
488(1)[0]	501(1)[11]	504(1)[2]	491(0.1)[5]	536(4)	535(5)	$\delta_{sciss}(SO_2)$	
487(0)[5]	498(0)[0]	503(0)[5]	487(1)[5]				
				458(2)			$\nu_{19}(F_2)$, $\delta(CN_4)$
				384(1)			$\nu_{12}(F_1)$, $\tau(CH_3)$
				370(1)	352(2)		
276(2)[8]	306(0)[15]	323(2)[6]	312(2)[5]	292(1)	310(5)		
261(1)[5]	281(5)[1]	308(4)[4]	276(3)[15]	231(7)	254(4)		
201(0)[10]	209(0)[16]	247(1)[3]	221(1)[9]		206(5)		
201(0)[15]	172(0)[3]	181(0)[8]	162(0.4)[2]	172(7)	183(4)		
140(0)[5]	131(0)[10]	146(1)[4]	139(0.4)[7]		161(14)		
135(1)[0]	130(2)[1]	112(0)[15]	109(0.1)[7]	128(10)	139(12)		
109(0)[1]	71(0)[4]	78(0)[4]	79(0.03)[9]		117(5)		
97(0)[2]	52(0)[3]	73(0)[6]	68(0.08)[6]	105(9)	105(11)		
71(0)[5]	20(0)[10]	34(0)[2]	45(0.01)[3]		89(5)		
47(0)[1]	19(0)[1]	30(0)[3]	26(0.05)[2]		78(5)		
					69(4)		
34(0)[0]	1(0)[1]	22(0)[0]	23(0.03)[2]		54(4)		

[a] Bands arising from the FEP sample tube were observed at 734(3) cm^{-1} for the $N(CH_3)_4(O_2S)_2N_3$ sample. [b] Raman spectra of $Cs(O_2S)_2N_3$ recorded at −130 °C on the Cary instead of the Bruker Equinox showed significant changes in the relative intensities of some of the bands.

tory if one keeps in mind that the skeletal modes involving the very long N−S bonds are strongly correlation dependent. Thus, the uncorrelated RHF method underestimates the bond length of the S−N bond resulting in high-frequency values for the modes involving the N−S bond. On the other hand, all the correlated methods significantly overestimate the S−N bond length (see Tables 4 and 5) resulting in low-frequency values for these modes. If one assumes that the actual bond lengths and frequencies fall between the uncorrelated and the correlated values, the fit between calculated and observed data becomes satisfactory. These results, together with our previous study of the SO_2F^- anion,[42] demonstrate the difficulties associated with the accurate calculation of highly ionic, long bonds. In view of the significant discrepancies between the observed and calculated frequencies, the calculated force fields have not been included in this paper.

$(SO_2)_2N_3^-$. Whereas the structure of the $SO_2N_3^-$ anion is firmly supported by its crystal structures, only Raman data are available for the $(SO_2)_2N_3^-$ ion. Because the negative charges in N_3^- are located on the two terminal nitrogen atoms

(42) Lork, E.; Mews, R.; Viets, D.; Watson, P. G.; Borrmann, T.; Vij, A.; Boatz, J. A.; Christe, K. O. *Inorg. Chem.* **2001**, *40*, 1303.

Table 8. Vibrational Spectra of [Cs][SO_3N_3]

vibrational frequencies, cm^{-1}				
exptl		calcd		assignments
IR, 22 °C	Raman, 22 °C	MP2	B3LYP	$SO_3N_3^-$ (C_s)
3337m				2134 + 1247 ($\nu_1 + \nu_{11}$)
2469m				1269 + 1247 ($\nu_3 + \nu_{11}$)
2450m				2 × 1247 (2 × ν_{11})
2283w				1247 + 1045 ($\nu_4 + \nu_{11}$)
2134vs	2138(23)	2272(19)[81]	2192(827)[89]	ν_1(A′), $\nu_{as}(N_3)$
	2118(15)			
1483w				2 × 744 (2 × ν_5)
	1278(8)	1285(1)[1]	1323(136)[8]	ν_2(A′), $\nu_s(N_3)$
1269vs		1283(9)[16]	1241(318)[14]	ν_3(A′), $\nu_{as}(SO_3)$
1247vs	1250(9)	1261(9)[7]	1218(336)[9]	ν_{11}(A″), $\nu_{as}(SO_3)$
1114w	1089(5)			
1045vs	1052(100)	1022(4)[44]	987(158)[40]	ν_4(A′), $\nu_s(SO_3)$
1028w				562 + 464 ($\nu_{13} + \nu_9$)
744s	746(18)	706(0.5)[5]	700(18)[5]	ν_5(A′), $\delta(N_3)$ in plane
640sh	644(10)	558(0.1)[0.1]	593(8)[0.1]	ν_{12}(A″), $\delta(N_3)$ out of plane
626vs		563(9)[7]	572(349)[6]	ν_6(A′), $\delta(SO_3)$ umbrella
618m				2 × 313 (2 × ν_4)
579w				
562s	558(13)	519(1)[4]	510(28)[4]	ν_{13}(A″), $\delta_{as}(SO_3)$
556s				
547s	550sh	518(0.5)[3]	509(18)[3]	ν_7(A′), $\delta_{sciss}(SO_2)$
464m	464(54)	363(2)[29]	369(34)[24]	ν_9(A′), ν(S−N)
	370(28)	314(1)[11]	314(11)[9]	ν_8(A′), $\delta_{rock}(SO_3)$
	364sh			
	313(8)	322(0)[1]	318(0)[1]	ν_{14}(A″), $\delta_{wag}(SO_3)$
	185(23)	123(0)[7]	139(1)[6]	ν_{10}(A′), δ_{sciss}(S−N−N)
	112sh			
		49(0)[6]	33(0)[6]	ν_{15}(A″), τ(S−N)

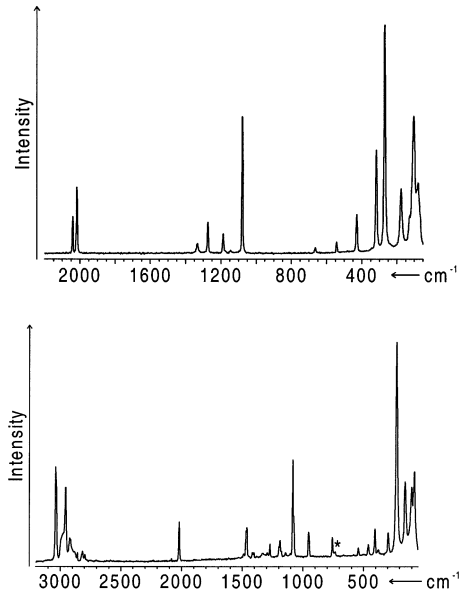

Figure 5. Raman spectra of $CsSO_2N_3$ (upper trace) and of $N(CH_3)_4SO_2N_3$ (lower trace). The band marked by an asterisk is due to the FEP sample tube.

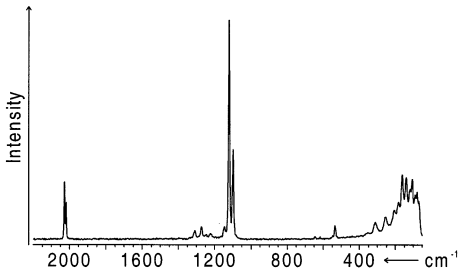

Figure 6. Raman spectrum of $Cs(SO_2)_2N_3$.

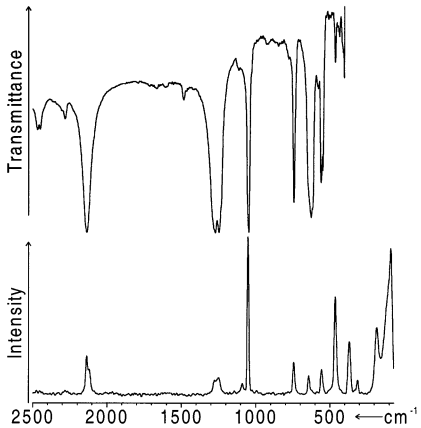

Figure 7. Infrared (upper trace) and Raman (lower trace) spectra of $CsSO_3N_3$.

(see previous discussion), the SO_2 groups must be attached to these. However, the two SO_2 groups could be attached to the same or to different nitrogen atoms. Theoretical calculations at the B3LYP and MP2 levels of theory (Figures 8 and 9) favor the geminal 1,1-$(SO_2)_2N_3^-$ over the terminal 1,3-$O_2SNNNSO_2^-$ adduct by 3.5 and 0.4 kcal/mol, respectively. Figure 8 also shows that the B3LYP and MP2 calculations result in very different minimum energy structures for the 1,3-adduct. At the MP2 level, there is, in addition to the N_α—S bond with 2.56 Å, also significant $\pi-\pi$ interaction between the N═N and S═O double bonds resulting in an N_β—O interaction of 2.84 Å, while at the B3YLP level the interaction occurs mainly through N−S bonds. Calculations were also carried out using the MP2 structure as the starting point for the B3LYP calculation and vice versa, but in each case, the calculations reverted

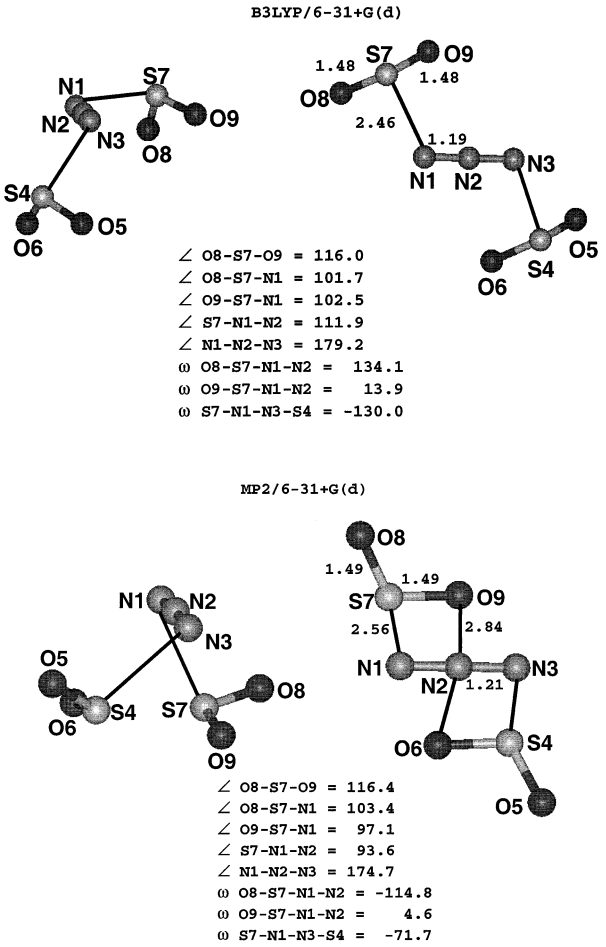

Figure 8. Structures of the 1,3-$(SO_2)_2N_3^-$ anion calculated at the B3LYP/6-31+G(d) and MP2/6-31+G(d) levels.

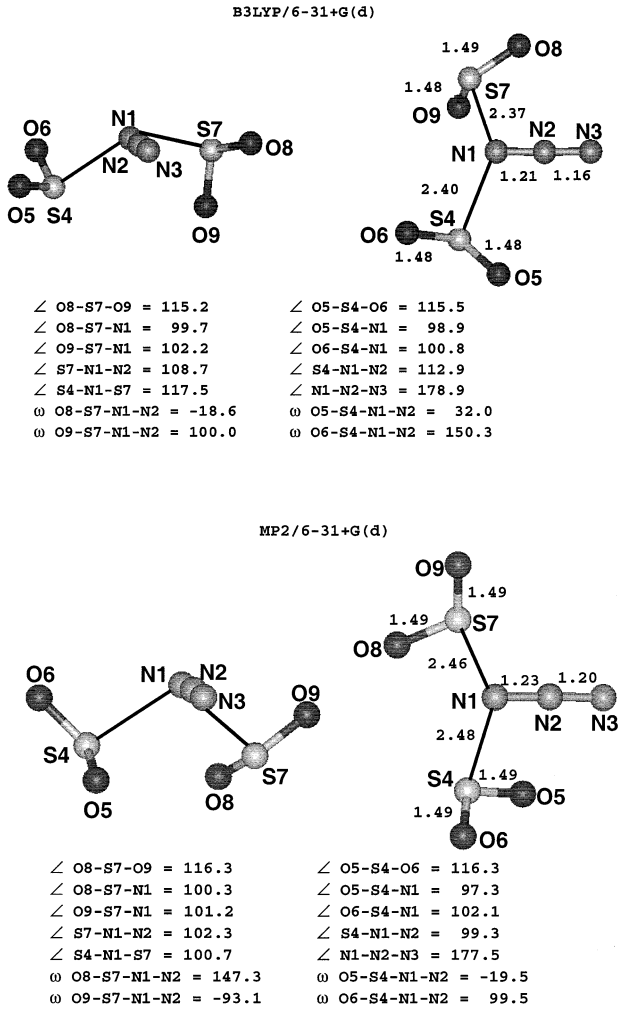

Figure 9. Structures of the 1,1-$(SO_2)_2N_3^-$ anion calculated at the B3LYP/6-31+G(d) and MP2/6-31+G(d) levels.

back to the structures shown in Figure 8, establishing that they are the true minima for each method. For the 1,1-adducts, the MP2 and B3LYP structures are more similar (Figure 9).

Distinction between the 1,1- and the 1,3-structures is possible from the observed Raman intensities (see Table 7). In the 1,3-structures, the relative intensities of the antisymmetric and the symmetric azide stretching modes are comparable, while in the 1,1-adducts, the antisymmetric stretching mode is much more intense than the symmetric one. Furthermore, in the 1,3-adduct, many of the low frequency skeletal modes are of low Raman intensity, while in the 1,1-adduct they are more intense and of comparable intensity. The observed spectra (see Table 7 and Figure 6) clearly favor the energetically preferred 1,1-structure.

SO_2 Solutions of N_3^-. The Raman spectra of the yellow solutions of N_3^- in liquid SO_2 show bands at about 2016(s) ($\nu_{as}N_3$), 1274(w) ($\nu_{as}SO_2$), 1120(vs) ($\nu_{sym}SO_2$), 646(mw) (δN_3), 400(br), and 230(br) cm^{-1} that are in accord with the spectra observed for the yellow, solid 1,1-$(SO_2)_2N_3^-$ adduct. In view of the similar spectra and the fact that the theoretical calculations indicate that the bonding of a third and fourth SO_2 ligand to $(SO_2)_2N_3^-$ becomes increasingly weaker (see previous discussion), the yellow species present in the N_3^-/SO_2 solutions is attributed to the 1,1-$(SO_2)_2N_3^-$ anion.

$SO_3N_3^-$. The structure of this anion is firmly established by the X-ray diffraction results (Figure 3). The theoretical calculations at the MP2 and B3LYP levels (see Tables 5 and 8 and Figure 3) result in almost identical geometries; however, compared to the experimental structure, the SO_3 group is rotated by 60° about the S−N axis. As for $SO_2N_3^-$, both methods significantly overestimate the N−S bond length, in this case by 0.12 Å. This bond distance overestimate results in an underestimate of those vibrational frequencies involving the S−N bond (see Table 8), but otherwise, the agreement between observed and calculated spectra is satisfactory. The fact that the S−N bond in $SO_3N_3^-$ is significantly shorter than that in $SO_2N_3^-$ has already been explained here by the increased Lewis acidity of SO_3. This increased withdrawal of electron density and negative charge from the azide anion in $SO_3N_3^-$ also causes a marked decrease in the N−N bond lengths, an increase in the average N_3 streching and bending frequencies, and an increased bond length difference between the $N_\alpha-N_\beta$ and $N_\beta-N_\gamma$ bonds.

Conclusions

The N_3^- anion acts as a pseudohalide and dissolves in liquid SO_2 forming yellow donor−acceptor adducts contain-

ing at least two SO_2 molecules per N_3^-. At low temperature, yellow $(SO_2)_2N_3^-$ salts can be isolated in which both SO_2 molecules are probably attached to the same terminal nitrogen atom. At about −30 °C, 1 mol of SO_2 can be pumped off, resulting in marginally stable, colorless $SO_2N_3^-$ salts that can be converted at about 50 °C into pure azides. The azidosulfites are analogous to the previously known azidosulfates but possess a significantly weaker S−N bond resulting in lowered thermal stability.

Acknowledgment. The authors thank Dr. Robert Corley for his steady encouragement and the National Science Foundation, the Defense Advanced Projects Agency, and the Air Force Office of Scientific Research for financial support. S.S. thanks the Alexander von Humboldt Foundation for a Feodor-Lynen fellowship, and M.G., the Natural Sciences and Engineering Research Council of Canada for a postdoctoral fellowship. This work was also supported in part by a grant of IBM SP time from the Aeronautical Systems Center at Wright-Patterson Air Force Base, a Department of Defense High Performance Computing Major Shared Resource Center.

Supporting Information Available: Tables of structure determination summary, atomic coordinates, bond lengths and angles, and anisotropic displacement parameters of $CsSO_2N_3 \cdot CsSO_3N_3$ in CIF format. This material is available free of charge via the Internet at http://pubs.acs.org.

IC020183L